Al-Nahrain Journal for Engineering Sciences (NJES) Vol.20 No.2, 2017 pp. 311-325
Special Issue - Proceedings of the 4th Eng. Conf. (21April 2016, Al-Nahrain Univ., Baghdad, IRAQ)
http://doi.org/10.29194/NJES20020311

Experimental and Numerical Investigation of High Strength Reinforced Concrete Deep Beams with Web Openings under Repeated Loading

Ihsan A. S. Al-Shaarbaf
Civil Eng. Dep.
Al-Nahrain University

Ahmed S. Ali
Civil Eng. Dep.
Al-Nahrain University
ahmed_sltn2007@yahoo.com

Abdulkhalik J. Abdulridha
Civil Eng. Dep.
Al-Nahrain University
abdulkalikjabbar@yahoo.com

Abstract

This paper presents experimental investigations to study the behavior of High Strength Reinforced Concrete (HSRC) deep beams with web openings under monotonic and static repeated loading conditions. The experimental work procedure consisted of testing eighteen simply supported HSRC deep beams both with and without web openings. The numerical work procedure consisted of testing ten simply supported HSRC deep beams both with web openings. All beams had the same dimensions and flexural reinforcement. They had an overall length of 1400 mm, a width of 150 mm and a height of 400 mm. The investigated test parameters were concrete compressive strength, shape and size of openings, vertical and horizontal reinforcement ratios, shear span to effective depth ratio (a/d ratio) and loading history. The experimental results reveal that the ultimate load capacities for specimens tested under four different repeated loading regimes decrease in the range between 2% and 19% in regards to the control specimens which were tested under monotonic loading regime. The results indicated that the increase in the severity of loading history leads to a decrease in the ultimate shear strength of the deep beams and causes increases in their ductility ratio. The ultimate loads of HSRC deep beams with square web openings size of (50*50mm, 60*60mm and 70*70mm) tested under the repeated loading history (HS-1) which consisting of five phases decreased by (11.4 %, 24.1% and 26.3 %, respectively) compared to that of identical solid deep beam. The ultimate load of HSCR deep beam with circular web openings shape tested under repeated loading history (HS-1) increases by 8.6 % compared to the equivalent square web openings shape. For numerically analyzed beams under repeated loading history (HS-1), the ultimate load increases by 16% when using area of 2500mm2 of circular web openings shape (equal in area to square web opening size 50mm*50mm) and by 13.5% when using rhombus web openings shape of the dimensions 50*50mm in comparison with the case of 60-mm size square web openings.

Keywords: Crack; cyclic loading; deep beams; high concrete strength; web openings**.**

1. Introduction

Pipes and ducts that intersect structural beams are necessary to accommodate essential services like water supply, sewage, air-conditioning, electricity, telephone, and computer network [1]. Transverse openings within ducts and pipes reduce the overall stiffness of such beams which may also give rise to excessive deflection under service load resulting in a considerable redistribution of internal forces and the strength of such geometries may also be reduced to a critical degree [2]. Web openings in deep beams cause geometric discontinuity within the beam and non-linear stress distributions over the depth of the beam [3]. The inclusion of web openings decreases the ultimate strength of a deep beam due to the reduction of concrete mass acting in compression and the opening acting as a stress raiser for shear crack propagation [4]. The American Concrete Institute AC1318M-11 [5] does not include specifications for web openings in deep beams. This has increased the need for a safe, accurate and uniform design methodology. Furthermore, the presence of openings produces discontinuities or disturbances in the normal flow of stresses. Hence the special reinforcement that enclose the opening at its periphery, should therefore be provided in sufficient quantity to control crack widths and prevent possible failure of the beam [6].

2. Experimental Program

The experimental program includes testing eighteen simply supported deep beams. All beams had the same dimensions and flexural reinforcement. The specimens have an overall length of 1400 mm, a width of 150 mm and a height of 400 mm which clearly indicates that the depth/thickness ratio of 2.7 adopted for all beams is quite safe with respect to the buckling behavior. The beams were designed to fail in shear. To bring about this type of failure, suitable flexural

reinforcing bars were provided to avoid premature flexural failure. A typical deep beam details in terms of geometry, reinforcement, load and support positions and other relevant parameters is shown in Figure (1). In all specimens, the amount of flexural bottom reinforcement for all the tested beams was 3Ø16mm diameter deformed steel bars widespread over the entire length of the beam and anchored adequately at the ends with 90 degree bends. The top reinforcement were (2Ø5 mm) diameter deformed steel bar. The beams were tested under two point symmetric loading with an overall clear span of 1140 mm which results in a ratio of clear span to overall depth that equals 2.85 which is less than 4.0 as recommended by the provisions of the ACI 318M-11 Code (4) for deep beam requirements. To overcome local failure due to crushing, steel bearing plates (Lb = 60 mm, width=150 mm, tb = 25 mm thickness) were seated at loading and reaction points. For web reinforcement, 5mm diameter deformed bars were used as vertical (closed stirrups) and horizontal side reinforcement. The length of all longitudinal reinforcement was 1350 mm with 75 mm of them extends on each side beyond the supports centerline and a vertical length of 300mm to make a 90 degree standard hook to provide sufficient anchorage. Both longitudinal and transverse steel bars were assorted and connected together by using (1 mm) steel wire. Spacers of 25mm were used at the sides of the deep beam to ensure adequate cover thickness and spacers of 50mm were used at the bottom of the deep beam to ensure adequate cover thickness. The objectives of this paper is to compute the effects of repeated loading scheme on the behavior of HSRC deep beams with web openings. Four types of repeated loading history (HS-1,HS-2, HS-3 and HS-4) are applied on the deep beams based on the results of the control specimen (DB-1) as shown in Figure (2). The repeated loading test depended on the displacement control investigation technique. For each cycle of loading, the displacement is gradually applied on the specimen until the required displacement level is reached. Then the applied displacement is gradually decreased to zero.

3. Experimental and Numerical Parameters

The experimental program was planned and executed to investigate the behavior of simply supported reinforced concrete deep beams with web openings under repeated loadings. The experimental program consists of casting and testing eighteen deep beams at the civil engineering laboratory of Al-Nahrain University. These beams were divided into groups depending on the (concrete compressive strength, shape and size of the openings, a/d ratio, vertical and horizontal reinforcement ratios, and loading history).The experimental program consists of testing eighteen deep beams with different parameters as shown in Table (1).

The parametric study presented in this paper consists of analyzing (10) deep beams which have been modeled using the damaged plasticity model presented in ABAQUS numerical program. The parameters considered in this numerical study are: flexural reinforcement ratio, both horizontal and vertical reinforcement bars ratio, vertical reinforcement ratios, circler web openings size and rhombus web openings size. All these specimens have a/d=1.2 and tested under loading history scheme (HS-1). The numerical program consists of testing ten deep beams under loading history (HS-1) with different parameters as shown in Table (2).

4. Finite Element Analysis of Deep Beam Specimens

All deep beams were modeled using three dimensional finite element. In ABAQUS [7] the standard 3D stress elements can be used to model the concrete. These elements are provided with the appropriate integration rules based on the experimental response of the specimen. Quadratic brick elements are chosen to provide higher precision for elements with strong distortions. These types of element capture stress concentrating better, and they are effective in bending and shear problems. The full 27(3x3x3) Gauss quadrature integration rule was chosen to represent the concrete. It is worth mentioning that the integration with quadratic order elements is favorite as they yield accurate results. Therefore the C3D20 (A 20-node quadratic brick element with full integration) elements are chosen to model the concrete. The reinforcing bars can be modeled by solid, beam and truss elements. The use of solid elements is computationally expensive and therefore was not chosen.

Truss elements are used because the reinforcing bars don't supply a very high bending stiffness. Perfect bond is assumed to occur between concrete and steel bars throughout the entire analysis. Therefore the T3D2 (A 2-node linear 3-D truss element) is used to model the reinforcing bars. Material modeling of concrete and most quasi-brittle materials is the compressive stiffness recovered upon crack closure as the load changes from tension to compression. On the other hand, the tensile stiffness is not recovered as the load changes from compression to tension once crushing micro-cracks have developed. This behavior, which corresponds to w_t=0 and w_c =1, is the default used by ABAQUS. Figure (3), illustrates a uniaxial load cycle assuming the default behavior. The three dimensional (3D)

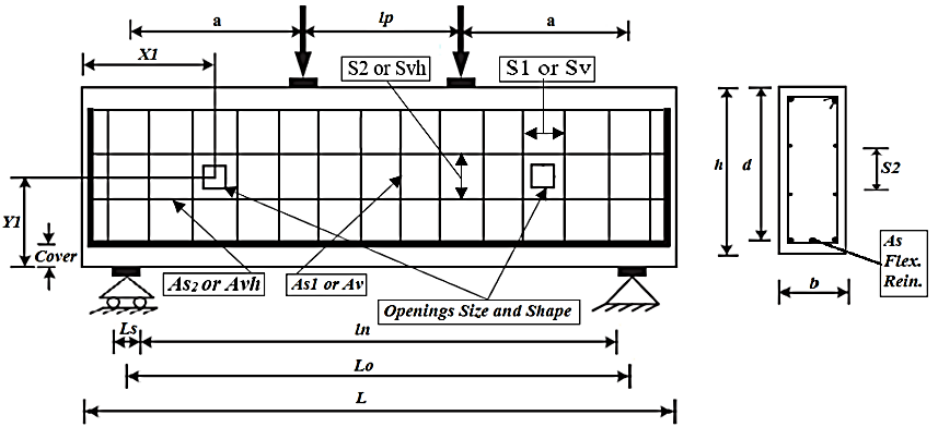

Figure 1: Typical deep beam details

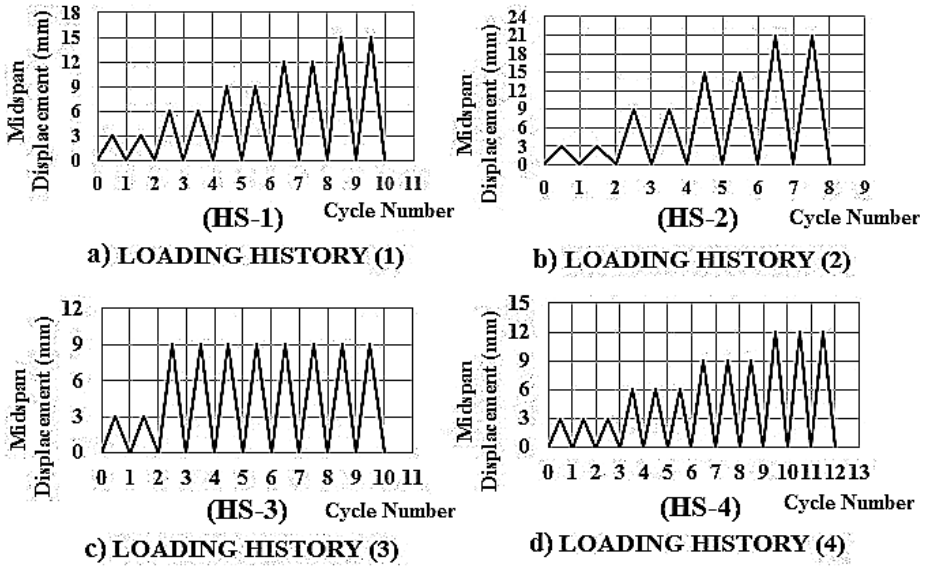

Figure 2: Loadings histories used in this research.

Table 1: Testing variables considered in experimental work.

Group No.	Beam designation	a/d ratio	Web opening shape	Web opening size	Loading History No. (HS)	Variable considered
1	DB-1	1.2	Square	60*60	-	Control specimens tested under monotonic loading
	DB-8	1.0	Square	60*60	-	
	DB-11	1.4	Square	60*60	-	
2	DB-2	1.2	Square	60*60	1	Repeated loading history
	DB-3	1.2	Square	60*60	2	
	DB-4	1.2	Square	60*60	3	
	DB-5	1.2	Square	60*60	4	
3	DB-2	1.2	Square	60*60	1	Shear-span depth ratio (a/d)
	DB-9	1.0	Square	60*60	1	
	DB-11	1.4	Square	60*60	1	
4	DB-2	1.2	Square	60*60	1	Concrete compressive strength (f'c)
	DB-6	1.2	Square	60*60	1	
5	DB-2	1.2	Square	60*60	1	Horizontal and vertical web reinforcement spacing
	DB-16	1.2	Square	60*60	1	
	DB-18	1.2	Square	60*60	1	
6	DB-2	1.2	Square	60*60	1	Vertical web reinforcement (ρv)
	DB-17	1.2	Square	60*60	1	
	DB-18	1.2	Square	60*60	1	
7	DB-2	1.2	Square	60*60	1	Web openings shape

	DB-14	1.2	Circle	60*60	1	
	DB-15	1.2	Rhombus	60*60	1	
8	DB-2	1.2	Square	60*60	1	Web openings size
	DB-12	1.2	Square	60*60	1	
	DB-13	1.2	Square	60*60	1	
9	DB-2	1.2	Square	60*60	1	Beams without web shear reinforcement
	DB-7	1.2	Solid	-	1	

Table 2: Properties for parametric study of numerical specimens.

Beam designation	(f´c) MPa	a/d	ρ_v %	ρ_h%	ρ_{main}	Web opening shape	Web opening size	Variable considered
DB-19	65	1.2	0.262	0.262	0.0088	Square	60*60	Flexural Reinforcement ratio
DB-20	65	1.2	0.262	0.262	0.018	Square	60*60	
DB-21	65	1.2	0.168	0.168	0.011	Square	60*60	Horizontal and vertical Reinforcement bars ratio
DB-22	65	1.2	0.377	0.377	0.011	Square	60*60	
DB-23	65	1.2	0.168	-	0.011	Square	60*60	Vertical reinforcement bars ratio
DB-24	65	1.2	0.377	-	0.011	Square	60*60	
DB-25	65	1.2	0.262	0.262	0.011	Circle	2500mm^2	Circle web openings area
DB-26	65	1	0.262	0.262	0.011	Circle	4700mm^2	
DB-27	65	1	0.262	0.262	0.011	Rhombus	50*50	Rhombus web Openings size
DB-28	65	1.4	0.262	0.262	0.011	Rhombus	70*70	

finite element meshes were adopted for the deep beam specimens are shown in Figure (4a). Quadratic brick elements are used to simulate the concrete and truss elements are used to simulate the steel bars. The bearing plates at top and bottom faces of the specimen are simulated by using quadratic elements (full contact element with full bond between bearing plates and the specimen). The applied load is subjected to a very slow displacement increment technique according to the selected loading history until failure. The applied boundary and loading conditions are shown in Figure (4b).

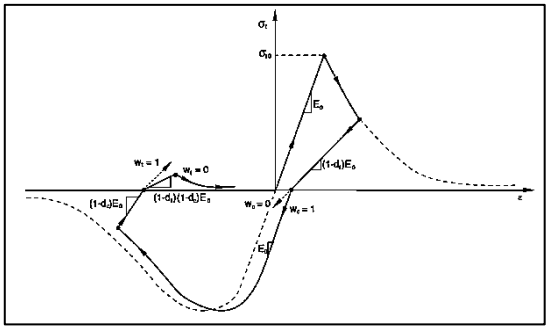

Figure 3: Uniaxial load cycle (tension-compression-tension) default values for the stiffness recovery factors: wt=0 and wc =1. [4

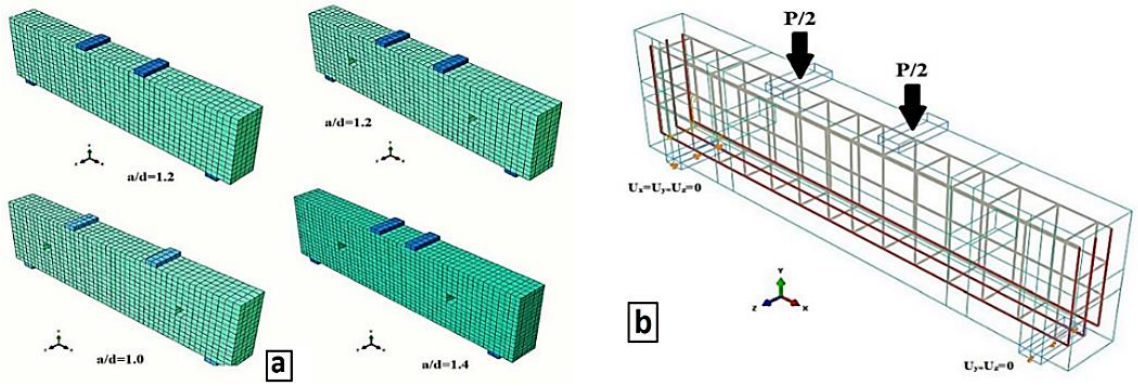

Figure 4: (a) Finite element meshes used to simulate of deep beam specimens, (b). Boundary and loading conditions used in the analysis.

4.1 Selected Model Parameters

The input data for the material properties models in the analysis are represented here. The stress strain curve for NS and HS concrete parameters are presented by Neville [8]. Figure (5) illustrates the tensile stress strain curves for

NS and HS concrete (peak tensile stress= fct , peak tensile strain= fct/Ec and ultimate strain=0.0002 as given by Neville (8)). The adopted analytical model for stress strain envelope curve for concrete subjected to axial cyclic compression was that given by Aslani and Jowkarmeimandi [9] as shown in Figure (6a) and Figure (6b). Aslani and Jowkarmeimandi proposed compressive stress– strain model for concrete under cyclic loading. The proposed envelope curve was commonly accepted by most researchers. The model has been verified experimentally and analytically. The input data for Aslani and Jowkarmeimandi analytical model are presented in Table (3) and Table (4). The plasticity damage model incorporated in ABAQUS requires the following input for computing the damage in concrete:

- Dilation angle, ψ.
- Flow potential eccentricity, e. The default of e =0.1 is usually used.
- σ_{b0} /σ_{c0} is the ratio of initial equibiaxial compressive yield stress to initial uniaxial compressive yield stress. The default of 1.16 is usually used.
- Kc, the ratio of the second stress invariant on the tensile meridian, q(TM), to that on the compressive meridian, q(CM) . The default of 2/3 is usually used.
- Viscosity parameter, μ , is used for the visco-plastic regularization of the concrete constitutive equations in ABAQUS Standard analyses. The default value is 0.0. (°C).

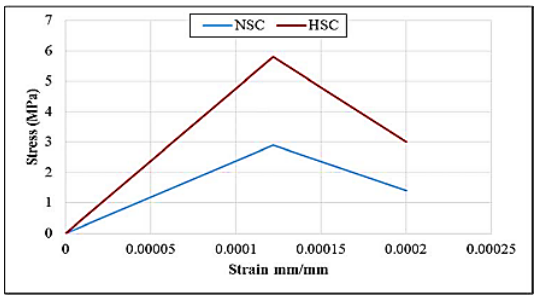

Figure 5: Tensile stress strain curve for NSC and HSC.

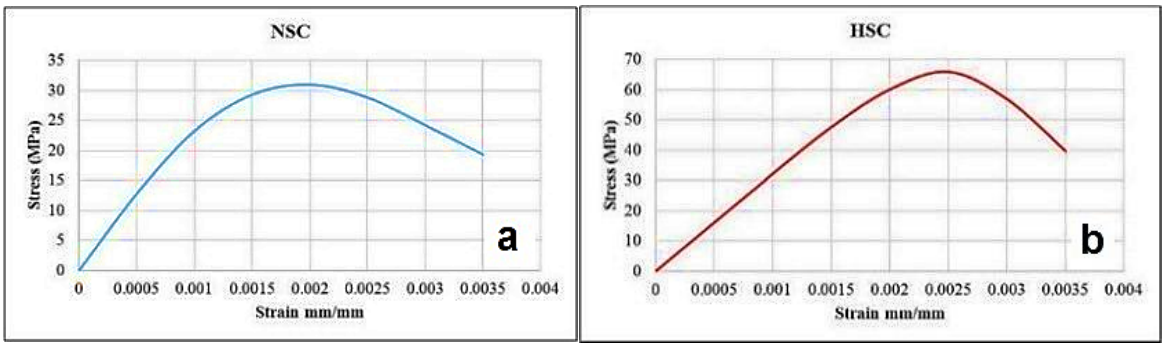

Figure 6: Stress strain curve (a) for NSC, (b) for HSC by using Aslani and Jowkarmeimandi model.

Table 3: Material properties of the FE model for reinforcing steel.

Parameter	Symbol	Units	Shear Reinf. (Ø 5)	Longitudinal Reinf. (Ø 16)	Parameter	Symbol	Units	Shear Reinf. (Ø 5)	Longitudinal Reinf. (Ø 16)
Elastic modulus	Es	(GPa)	200.1	200.6	Ultimate stress	fu	(MPa)	729	742
Poisson´s ratio	υ	-	0.3	0.3	Yield strain	ε_{sy}	mm/m	0.00329	0.00236
Density	ρ	kg/m^3	7850	7850	Strain at ultimate	ε_{su}	mm/m	0.063	0.114
Yield stress	fy	(MPa)	658	474					

Table 4: Material properties of the FE model for concrete.

Parameter	Symbol	Units	Value	Remarks
Elastic modulus	Ec	(GPa)	-	Table (3)
Poisson´s ratio	υ	-	0.2	Ref. [8]
Density	ρ	kg/m3	2400	-
Compressive cylinder strength	f´c	(MPa)	-	Table (3)
Compressive strain at peak	ε_c	mm/mm	0.0002	Ref. [8]
Tensile strength	f_{ct}	(MPa)	-	Table (3)
Dilation angle	ψ	°	36	-
Maximum limit of damage	d max	-	0.9	-
Inelastic strain of concrete in compression	ε_c^{in}	-	0.0005 to 0.0035 (NSC) 0.0008 to 0.0035 (HSC)	Figure (4)
Cracking strain of concrete in tension	ε_t^{ck}	-	0.0002	Figure (4)

5. Results

The experimental program consists of testing eighteen reinforced concrete deep beams with web openings. Fifteen specimens were subjected to repeated loading system and the remaining three specimens have been subjected to monotonic static loads. The specimens tested under monotonic loading had the same properties except the value of a/d ratio. These beams were provided with steel stirrups arranged in both horizontal and vertical directions. The summary of test results of all specimens are shown in Table (5). The failure modes for all tested specimens are shown in Plate (1). One of the most important aspects that must be recognized during testing the deep beam specimens under the applied load is the load-midspan deflection curve. The load-midspan deflection curves for the all specimens under the various parameters and test conditions are shown in Figure (7).

5.1 Numerical Analysis of the Parametric Study Specimens

Finite element models using ABAQUS software program (ABAQUS-12.1) were developed to simulate the behavior of HSRC deep beams with web openings under monotonic and repeated loading schemes. The experimental results of specimens were adopted as verification problems for deep beams under repeated loadings history. Aslani and Jowkarmeimandi proposed models to predict behavior of concrete in compression and in tension they were adopted. In the present numerical model, the model reveals that the computer program results are in good agreement of load versus midspan deflection and good agreement between numerical and experimental results. The finite element results can be used as a guidance to explore the reinforced concrete response under different properties and loading conditions.

The parametric study presented in this paper consists analyzing of ten deep beams which have been modeled using the plasticity damage model presented in ABAQUS Numerical program. The parameters considered in this numerical study are: flexural reinforcement ratio, both horizontal and vertical reinforcement bars ratio, vertical reinforcement ratios, circular web openings size and rhombus web openings size. All these specimens have a/d=1.2 and tested under loading history scheme (HS-1).

The numerical results for ultimate loads and the corresponding displacements for the numerically analyzed deep beams is given in Table (6). Numerical crack pattern and zones of concrete cracking and crushing damages after analyzing all parametric study specimens are shown in Figure (8). Numerical load-displacement responses for these specimens are shown in Figure (9)

.

Table 5: Summary of test results of deep beam specimens.

Group No.	Beam designation	a/d ratio	Web opening shape	Web opening Size	f´c (MPa)	fct (MPa)	Ec (Gpa)	First Crack Load (kN)	Failure Load (kN)	First Crack displacement (mm)	Failure displacement (mm)	Loading history No.	Variable considered
1	DB-1	1.2	Square	60*60	67.1	5.8	35.7	221.3	562.5	4.8	11.6	Mono.	Control specimens (monotonic loading)
	DB-8	1.0	Square	60*60	64.0	5.6	33.9	225.5	641.4	5.3	11.0	Mono.	
	DB-11	1.4	Square	60*60	65.6	5.2	32.4	192.3	561.3	5.1	12.3	Mono.	
2	DB-2	1.2	Square	60*60	66.8	5.7	35.6	216.5	551.4	4.5	12.0	1	Repeated loading history
	DB-3	1.2	Square	60*60	64.1	5.6	33.5	210.3	480.8	4.5	11.1	2	
	DB-4	1.2	Square	60*60	62.0	5.4	32.2	187.2	499.4	4.1	11.7	3	
	DB-5	1.2	Square	60*60	65.4	5.6	33.6	169.7	455.9	3.6	9.8	4	
3	DB-2	1.2	Square	60*60	66.8	5.7	35.6	216.5	551.4	4.5	12.0	1	Shear-span to effective depth ratio (a/d)
	DB-9	1.0	Square	60*60	67.6	5.9	35.5	217.9	622.1	4.5	12.0	1	
	DB-10	1.4	Square	60*60	62.6	5.4	31.4	171.3	527.2	4.0	12.9	1	
4	DB-2	1.2	Square	60*60	66.8	5.7	35.6	216.5	551.4	4.5	12.0	1	Concrete compressive strength (fc´)
	DB-6	1.2	Square	60*60	30.9	2.7	25.1	145.8	411.3	3.4	9.8	1	
5	DB-2	1.2	Square	60*60	66.8	5.7	35.6	216.5	551.4	4.5	12.0	1	Horizontal and vertical web reinforcement
	DB-16	1.2	Square	60*60	62.5	5.7	32.3	173.1	495.2	3.4	9.3	1	
	DB-18	1.2	Square	60*60	66.5	5.5	34.7	113.4	389.9	3.3	8.1	1	
6	DB-2	1.2	Square	60*60	66.8	5.7	35.6	216.5	551.4	4.5	12.0	1	Vertical web reinforcement (ρv)
	DB-17	1.2	Square	60*60	64.3	5.6	33.4	191.2	515.8	4.2	11.1	1	
	DB-18	1.2	Square	60*60	66.5	5.5	34.7	113.4	389.9	3.3	8.1	1	
7	DB-2	1.2	Square	60*60	66.8	5.7	35.6	216.5	551.4	4.5	12.0	1	Web openings shape
	DB-14	1.2	Circle	60*60	65.3	5.7	33.6	230.9	598.8	5.1	12.8	1	
	DB-15	1.2	Rhombus	60*60	64.4	5.7	33.5	213.9	580.1	5.3	13.7	1	
8	DB-2	1.2	Square	60*60	66.8	5.7	35.6	216.5	551.4	4.5	12.0	1	Web openings size
	DB-12	1.2	Square	50*50	64.1	5.5	32.6	230.5	644.2	5.6	12.8	1	
	DB-13	1.2	Square	70*70	67.2	5.4	35.8	173.0	535.8	4.1	11.2	1	
9	DB-2	1.2	Square	60*60	66.8	5.7	35.6	216.5	551.4	4.5	12.0	1	Without web openings
	DB-7	1.2	Solid	-	66.7	5.8	35.5	196.3	727.2	5.5	13.3	1	

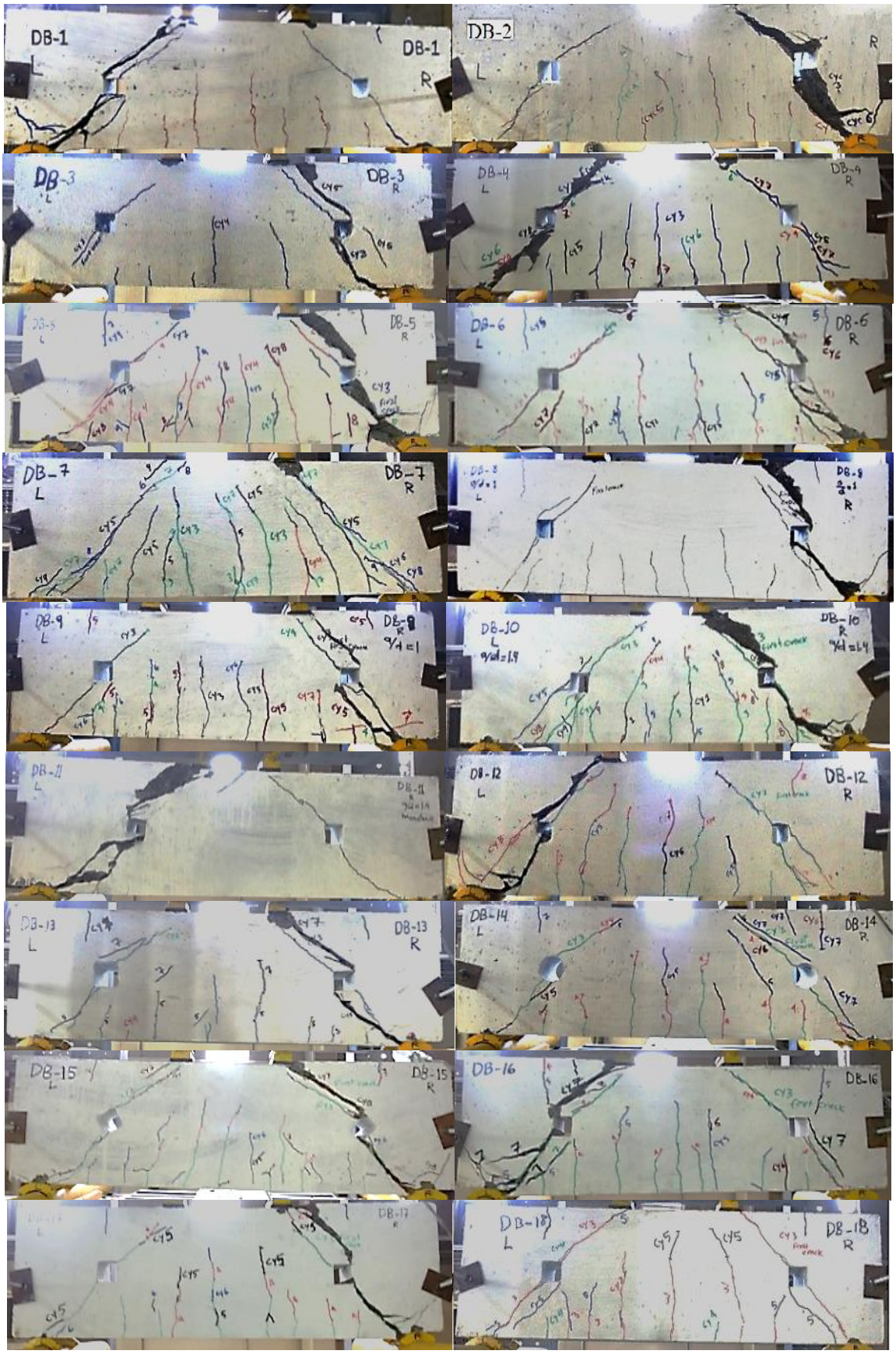

Plate 1: Failure modes after testing for all specimens.

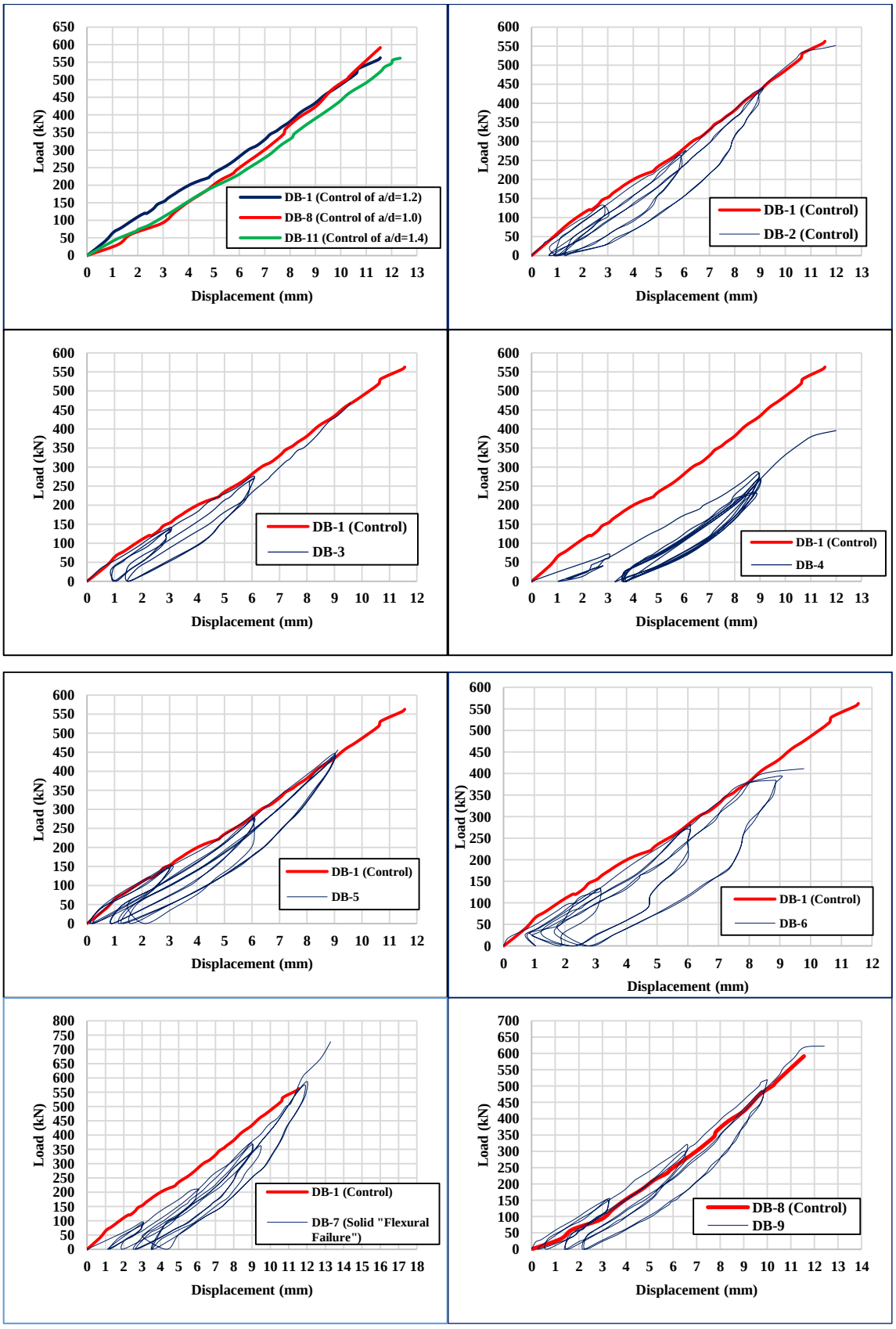

Figure 7: Load-midspan deflection curves for all tested specimens.

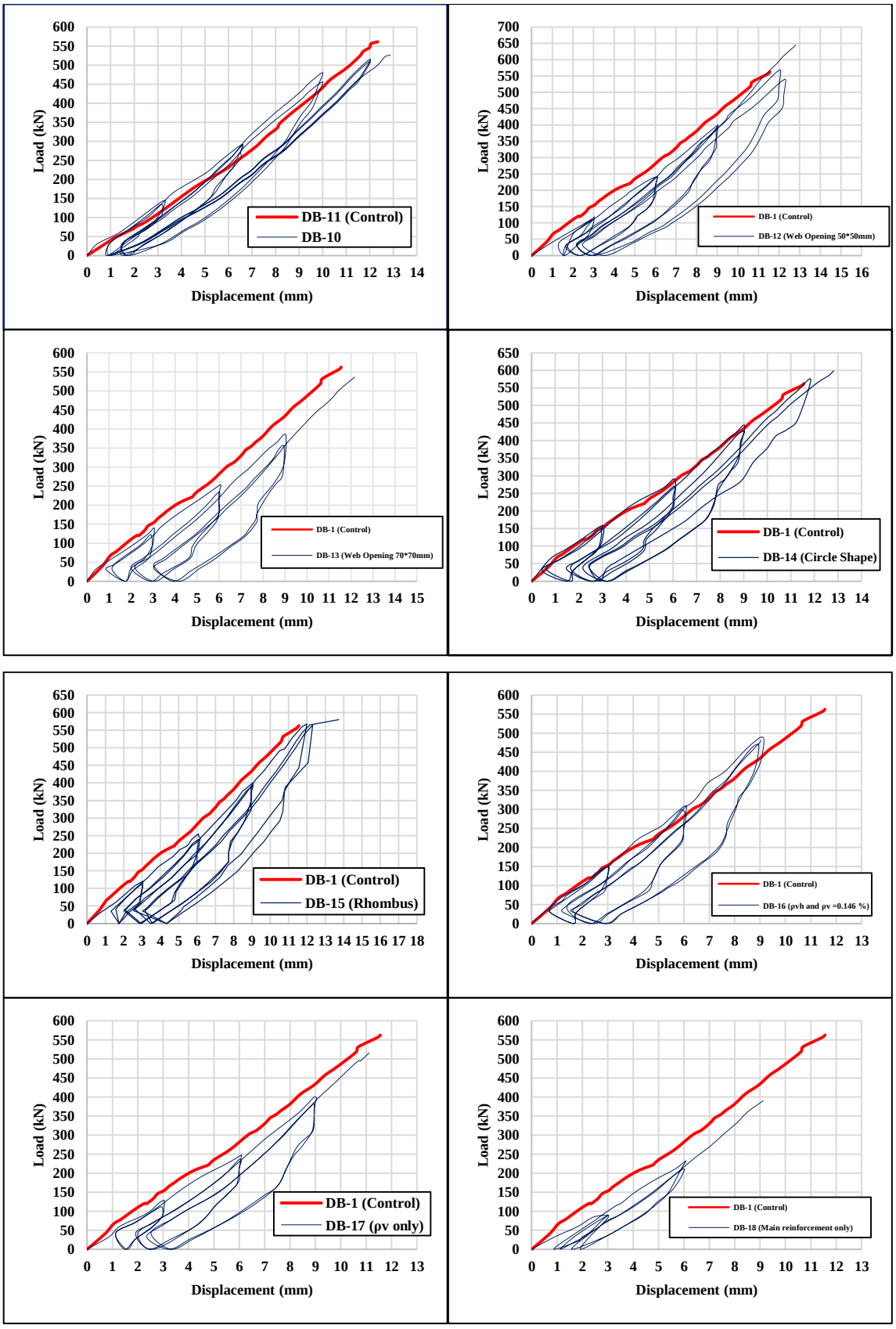

Figure 7: continued.

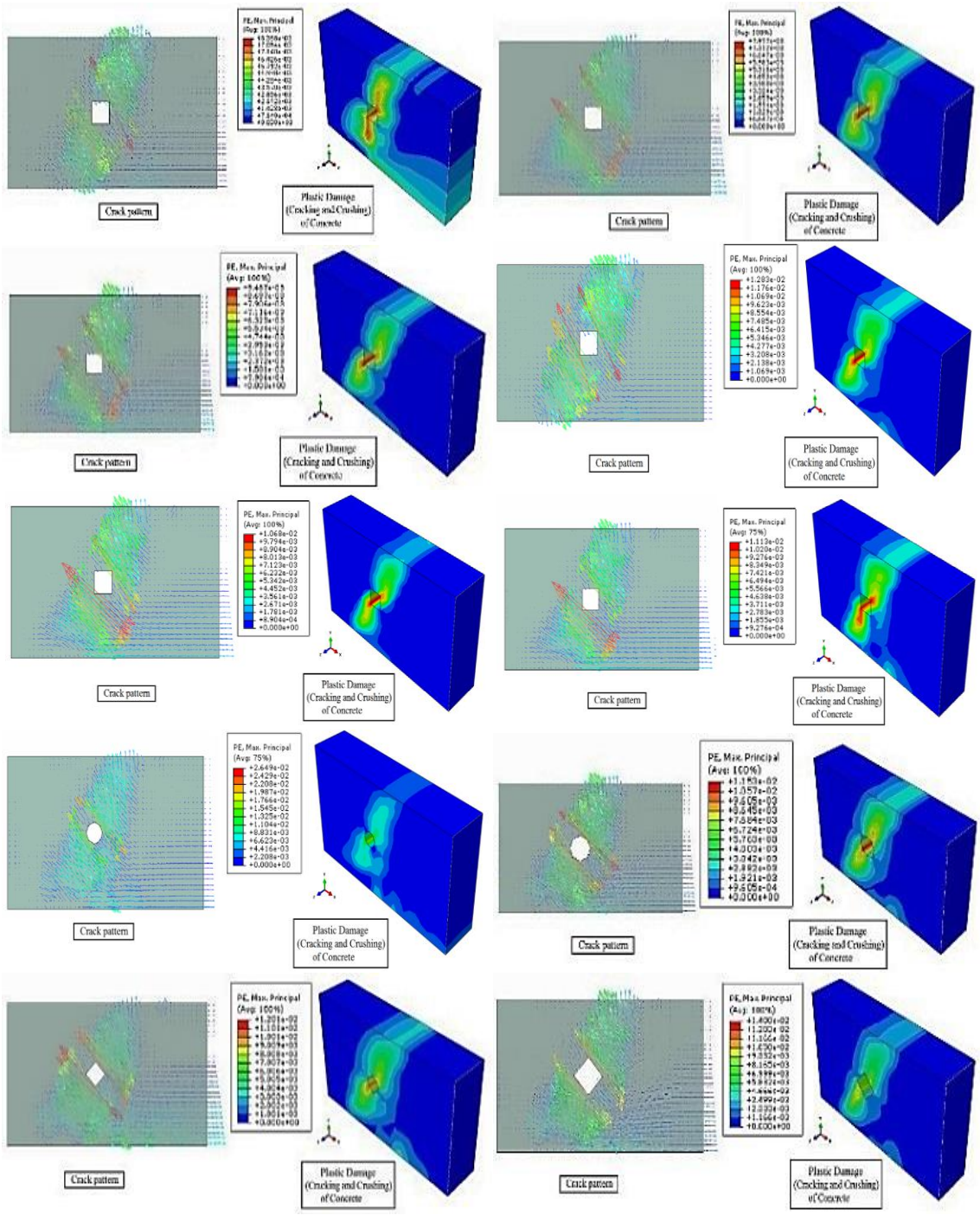

Figure 8: Numerical crack pattern and zones of concrete cracking and crushing damages after analyzing all parametric study specimens.

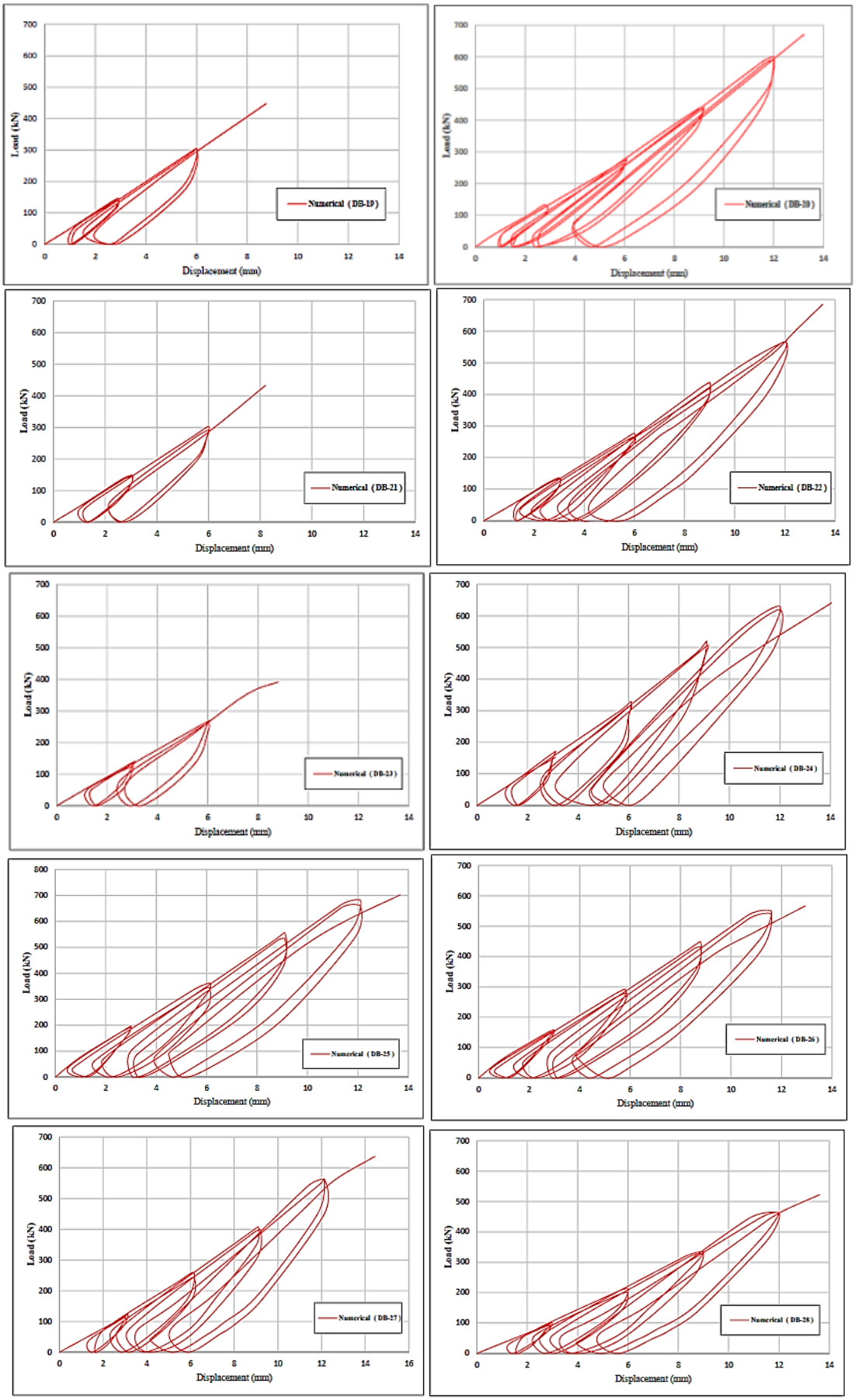

Figure 9: Load-midspan deflection curves for all numerical specimens.

Table 6: Results of the numerically analyzed specimens.

Beam designation	Deep beam properties considered	Numerical results		Numerical cycle at failure	Variable considered
		Ultimate load (kN)	Corresponding displacement (mm)		
DB-2	3Ø16	535.9	12.7	9	Flexural reinforcement ratio
DB-19	3Ø14	447.4	8.7	5	
DB-20	3Ø20	667.3	13.2	9	
DB-2	ρv = ρvh =0.262%	535.9	12.7	9	Horizontal and vertical reinforcement bars ratio
DB-16	ρv = ρvh =0.131%	480.2	10.1	7	
DB-18	ρv = ρvh = 0.0%	366.7	9.8	7	
DB-21	ρv = ρvh =0.168%	432.5	8.2	5	
DB-22	ρv = ρvh =0.377%	685.3	13.5	9	
DB-17	ρv =0 and ρvh =0.262%	508.9	11.8	7	Vertical reinforcement bars ratio
DB-23	ρv =0 and ρvh =0.168%	391.7	8.8	5	
DB-24	ρv =0 and ρvh =0.377%	643.2	13.6	9	
DB-14	Opening size=3600mm2	589.3	13.4	9	Circle web openings size
DB-25	Opening size=2500mm2	702.7	13.7	9	
DB-26	Opening size=4900mm2	566.8	12.9	9	
DB-15	Opening size=60*60mm	550.8	14.2	9	Rhombus web openings size
DB-27	Opening size =50*50mm	636.9	14.4	9	
DB-28	Opening size =70*70mm	522.7	13.6	9	

6. Conclusions

The following conclusions are drawn from the experimental and numerical investigation:

1. The ultimate load capacity for HSRC deep beams with web openings tested under repeated loading schemes (HS-1), (HS-2), (HS-3) and (HS-4) decrease in the range between 2 % and 19 % in regards to the monotonically loaded control specimen (DB-1). This means that the increase in the severity of loading history leads to an increase in the ultimate shear strength of deep beams.
2. The ultimate load of HSRC deep beam with web openings tested under repeated loading history (HS-1) increases by 27.3% when both horizontal and vertical web reinforcement ratio are increased from ρ_{vh} and ρ_v =0.0% to 0.131%. Also it can be noted that the increase in both horizontal and vertical web reinforcement ratio from ρ_{vh} and ρ_v =0.0% to 0.262 % leads to an increase in the ultimate load by 41.4 %. This means that the increase in both longitudinal and transverse reinforcement ratios leads to an increase in the ultimate load of HSRC deep beam with web openings tested under repeated loading.
3. The ultimate load of HSRC deep beam with circular web openings shape tested under repeated loading history (HS-1) is increased by 8.6 % when compared to deep beam having square web openings shape with the same opening area. Also the ultimate load of HSRC deep beam with rhombus web openings shape tested under repeated loading history (HS-1) is increased by 5.1% compared to deep beam with square web openings shape having the same area.
4. The ultimate load of HSRC deep beam with square web openings size 50*50mm tested under repeated loading history (HS-1) decreases by 11.4 % when compared to that of an identical solid deep beam. Meanwhile, the ultimate load of HSRC deep beam with square web openings size 60*60mm tested under repeated loading history (HS-1) decreases by 24.1% when compared to an identical solid deep beam. Also the ultimate load of HSRC deep beam with square web openings size 70*70mm decreases by 26.3 % when compared to an identical solid deep beam.
5. The finite element model predicts the experimental response under repeated loading up to the yielding of steel bars. Then the predicted results were slightly less accurate during the inelastic range. The models implemented in the ABAQUS computer program can accurately predict the region of damage within the HSRC deep beams. The crack patterns obtained for the analyzed specimens under monotonic and repeated loading schemes using the finite element models are similar to the crack patterns occurred in the experimental work.

6. The numerical behavior of deep beams represented by the load- displacement curve under monotonic loading scheme shows an acceptable agreement with the corresponding experimental curves.
7. For numerically analyzed beams under repeated loading history (HS-1), the ultimate load capacity decreases by 16.5% when using 3ϕ14mm as main longitudinal bars instead of 3ϕ16mm, while the numerical ultimate load increases by 24.5% when using 3ϕ20mm as main longitudinal bars.
8. For numerically analyzed beams under repeated loading history (HS-1), the ultimate load capacity decreases by 3.8% when using 4900mm2 circular web openings shape (equal in area of square web opening size 70mm*70mm) instead of 3600mm2 circular web openings shape. However, the numerical ultimate load increases by 16% when using 2500mm2 circular web openings shape (equal in area of square web opening size 50mm*50mm).
9. For numerically analyzed beams under repeated loading history (HS-1), the ultimate load capacity decreases by 5.1% when using rhombus web openings shape with size 70mm*70mm instead of rhombus web opening size 60mm*60mm and the numerical ultimate load increases by 13.5% when using rhombus web openings shape with size 50mm*50mm.

ACKNOWLEDGMENT

The work presented in this paper was supported by Official Research and Development Department \ Department of Entrepreneurial Project Management. The authors gratefully acknowledge the contributions of Official Research and Development Department \ Department of Entrepreneurial Project Management.

References

[1] Mansur M. A. and Kiang-Hwee Tan., "Concrete beams with openings: analysis and design", Boca Raton, Florida, CRC Press LLC, 1999, 220 pp.

[2] Jin-Seop Lee and Sang-Sik Kim, " Shear Behavior of Reinforced Concrete Deep Beams with Web Openings ", Journal of the Korea Concrete Institute, Vol. 13, No. 6, 2001, pp. 619-628.

[3] Guan, H. and Doh, J. H., "Development of Strut-and-Tie Model in Deep Beams with Web Openings", Journal of Advances in Structural Engineering, Vol. 10, No. 6, 2007, pp. 697-711.

[4] Kong, F. K. and Sharp, G. R., "Structural idealization for the deep beams with web openings", Magazine of Conc. Rese., Vol. 29, No. 99, 1977, pp. 81-91.

[5] ACI Committee 318, "Building Code Requirements for Structural Concrete (318-11) and Commentary (318-11) ", American Concrete Ins., Detroit, 2011.

[6] Mansur MA, Tan KH, Lee SL., "Collapse loads of RC beams with large openings", ASCE Str. Eng. Journal, Vol.110, No. 11, 1984, pp. 2602–10.

[7] ABAQUS," Abaqus 6.12 Abaqus/CAE User's Manual", Inc., 2012, available at http://www.maths.cam.ac.uk/computing/software/abaqus_docs/docs/v6.12 /pdf_books CAE.pdf".

[8] Neville, A.M., "Properties of Concrete", the English Language Book Society & Pitman Publishing, 3rd Edition, 1983, 566 pp.

[9] Aslani, F. and Jowkarmeimandi R., "Stress-strain model for concrete under cyclic loading", Magazine of Concrete Research, Vol. 64, No.8, 2012, pp.673-685.

التحقيقات التجريبية و العددية للعتبات الخرسانية المسلحة العميقة ذات الفتحات في وتراتها تحت تحميل المتكررة

احسان علي صائب
قسم الهندسة المدنية
جامعة النهرين

احمد سلطان علي
قسم الهندسة المدنية
جامعة النهرين

عبد الخالق جبار عبد الرضا
قسم الهندسة المدنية
جامعة النهرين

الخلاصة

يهدف هذا البحث الى التحري التجريبي والتحليلي عن لدراسة سلوك العتبات الخرسانية المسلحة العميقة عالية المقاومة الحاوية على فتحات في وتراتها المعرضة الى الأحمال التزايدية التكرارية باتجاه واحد. يتألف البرنامج العملي التجريبي من فحص ثمانية عشر من العتبات الحاوية وغيرالحاوية على فتحات في وتراتها. كما كانت جميع النماذج ذات ابعاد (طول 1400 ملم, سماكة 150 ملم و ارتفاع 400 ملم). فحصت النماذج تحت تأثير ازاحة استاتيكية تزايدية تكرارية باتجاه واحد. اشتملت متغيرات البحث على مقاومة انضغاط الخرسانة و شكل وحجم الفتحات و نسبة حديد التسليح الشاقولي والافقي و نسبة فضاء القص الى الارتفاع الفعال للعتبة وانماط التحميل التكراريةأربعة انماط من التحميل المتكرر سلط على العتبات العميقة مستندة على نتائج فحص النموذج المتحكم. أظهرت النتائج التجريبية انخفاض التحمل الاقصى لهذه العتبات بنسب تتراوح بين 2% و19% نسبة الى النموذج المفحوص تحت تحميل تزايدي بأتجاه واحد .هذا يعني ان الزيادة في شدة نمط التحميل المتكرر تؤدي الى تقليل مقاومة القص للعتبات العميقة.